Contract No.:

This manuscript has been authored by Savannah River Nuclear Solutions (SRNS), LLC under Contract No. DE-AC09-08SR22470 with the U.S. Department of Energy (DOE) Office of Environmental Management (EM).

Alpha Air Sample Counting Efficiency versus Dust Loading: Evaluation of a Large Data Set

MG Hogue* , SM Gause-Lott, BN Owensby, TM Slack, JJ Smiley, JL Burkett

Abstract –Dust loading on air sample filters is known to cause a loss of efficiency for direct counting of alpha activity on the filters, but the amount of dust loading and the correction factor needed to account for attenuated alpha particles is difficult to assess. In this paper, correction factors are developed by statistical analysis of a large database of air sample results for a uranium and plutonium processing facility at the Savannah River Site. As is typically the case, dust loading data is not directly available, but sample volume is found to be a reasonable proxy measure; the amount of dust loading is inferred by a combination of the derived correction factors and a Monte Carlo model.

The technique compares the distribution of activity ratios (beta/(beta + alpha) by volume and applies a range of correction factors on the raw alpha count rate. The best-fit results with this method are compared with MCNP modeling of activity uniformly deposited in the dust and analytical laboratory results of digested filters. A linear fit is proposed to evenly-deposited alpha activity collected on filters with dust loading over a range of about 2 mg·cm^{-2} to 1000 mg·cm^{-2}.

Key words: air sampling, aerosols, alpha particles, Monte Carlo

Sources of Funding: The authors declare no conflicts of interest. Authors are funded by the United States Department of Energy via the Management and Operations Contract for the Savannah River Site.

INTRODUCTION

Occupational airborne radioactivity monitoring at the Savannah River Site (SRS) covers a range of facilities and source terms including actinide processing and storage, high level nuclear waste storage and treatment, as well as a variety of laboratory facilities. Data from the air sampling program has been compiled over a period of 13 years into a database containing over 800,000 results at the time of evaluation. The total for this evaluation was a subset for a uranium and plutonium processing facility containing 297,349 sample results. Most of the air sample results (55%) show no activity above background. The beta activity is predominantly from fission products, ^{137}Cs and $^{90}Sr/^{90}Y$.

The results span a large range of volumes, up to 1500 m^3 on 47 mm diameter glass fiber filters. Samplers are routinely run at a flow rate averaging 0.0566 $m^3\,min^{-1}$. Sample collection frequencies occur at various intervals such as twice per week, weekly and biweekly. Sample collection frequency can be impacted by personnel scheduling, facility operations and cost-saving efforts intended to reduce the numbers of samples counted.

Counting alpha radioactivity on air filters depends on many parameters that can impact the alpha particles reaching and being counted by the detector. In a typical low level alpha/beta gas proportional counting system*, a successfully counted alpha particle has to have a trajectory out of the filter in the direction of the detector. It must retain enough energy to get through a window, if applicable to the counting system – the Canberra 5 XLB used on these samples includes a window that is 80 $\mu g \cdot cm^{-2}$ thick – and have enough energy to be recognized as alpha radiation, rather than beta or photon radiation.

Previous studies on alpha activity on air sample filters have highlighted a range of factors that affect counting results. Filter penetration issues have been studied by Billard et. al. 1967, Higby 1984, Luetzelschwab et. al. 2000, and Geryes et. al. 2007, 2009-a and 2009-c. When a particle is embedded in a filter, alpha particles may be attenuated before they get to the detector. These studies, and Geryes 2009-b, were used to develop the Monte Carlo model in this study for lightly loaded air samples.

The mass of a host dust particle provides another attenuating effect. For example, a large dust particle of 5 μm aerodynamic median air diameter (AMAD) has more self-attenuation than a small dust particle of 1 μm AMAD. Pickering 1984, Huang et. al. 2002 and Geryes et. al. 2008 and Geryes 2009-a discuss loss of efficiency due to particle size. Since this study does not distinguish correction factor by particle size, the effect of this self-attenuation is captured, along with filter self-absorption, in the ratio to analytical laboratory results discussed below.

Dust loading on the filter often provides the most significant attenuation, as is the case with the samples analyzed here. Overall corrections for dust loading are covered in Barnett et. al. 2009, Geryes et. al. 2009-a, 2009-b and 2011. The difficulty of assessing dust loading by direct measurements of samples is discussed in Barnett et. al. 2009.

Sample representativeness and collection efficiency (Hinds 1999, Maiello and Hoover 2011, Whicker 2003, Hogue et. al. 2014) are separate issues, beyond the scope of this paper. Reductions in collection efficiency due to filter clogging (Hinds 1999) must be mentioned at least as a contributor to the uncertainty in the slope of the correction factors, and conversion from total flow to dust loading in Figure 3.

---

* The Savannah River Site is using Canberra Series 5 XLB Automatic Low Background Alpha /Beta Counting System, User Manual # C39349, Canberra Industries; November 2013.

The goal of this paper is to develop correction factors based on trends in alpha and beta activity that are observed with larger collection volumes. It starts with the tentative assumption that since the air samples are collected in a facility with a reasonably consistent set of radionuclides present, the expected distribution of alpha and beta activity should be similar unless affected by the larger volumes. Correction factors are sought that will account for attenuation of alpha particles in the dust layer that grows thicker with longer sample volumes. Proposed correction factors are tested based on their success in producing a match of the distribution of activity ratios in a select population of higher volume samples to the distribution of activity ratios of the base, low volume samples. A goodness of fit test (Gareth et. al. 2013) is used to check the corrected activity distribution against the base distribution.

Monte Carlo modeling of ^{238}Pu particles in air sample filters with varying layers of dust was performed using MCNP 6 (Goorley et. al. 2012). This modeling was used to estimate the dust loading in the sample results.

Validity of the correction factors derived here depend on key assumptions. These assumptions are: 1) Radioactivity is deposited uniformly over time. 2) The mass concentration and elemental composition of the dust are consistent. 3) The distribution of sources of radioactivity (e.g. actinides and fission products) collected on the samples is the same over time. Situations that would cause these correction factors to be inaccurate include: 1) Higher air activity early in the collection period would be masked by later deposits, causing a low bias, while higher air activity late in collection time would cause a high bias. 2) A change in facility operation or environmental condition such as dust-producing activities, fires, grinding, etc., could produce variations in the quantity and attenuating quality of the dust. 3) Facility operations can vary, releasing more or less of a particular radionuclide. Despite the variability in the overall sample population, application of the correction factors plausibly matched the distributions of air activity ratios of low volume samples to sample populations from a large range of higher volume samples.

MATERIALS AND METHODS

Air sample data was collected from the database relating to a uranium and plutonium facility. The counting data was restricted to samples that were decayed greater than five days (to avoid the influence of ^{220}Rn decay progeny). Bayesian estimates of alpha and beta activity were used (Strom et. al. 2012, Labone and Chalmers 2014). Alternative treatments, such as censoring zero alpha count data points (which includes two thirds of the samples) were evaluated, and found to have no impact on results.

A ratio was computed for each sample by dividing the beta activity by the sum of uncorrected alpha and beta activity. This ratio provided a metric with a convenient range from 0 to 1. As alpha particles are removed by excess dust, the ratio moves to a higher proportion of ratios close to 1 (Figure 1). The ratio results were partitioned into volume categories corresponding to sampling intervals. Figure 1 provides a boxplot of the ratios. The center horizontal line of each box is the median, the first and third quartile lines form the bottom and top of the box, and the extending vertical lines provide a measure of the range of data below and above the first and third quartiles.

The method of estimating the additional correction factor for excess dust loading is to match the distribution of the ratio described above (beta activity to the sum of the beta and alpha activity) from the higher volume samples to the lowest volume samples. As the volume increases, the distribution of the beta/(beta + alpha) ratio changes dramatically. The top two charts in Figure 2 provide comparative distributions before correction. As alpha particles are lost to dust loading, there are fewer alphas in the denominator of this ratio. The method assumes that the true distribution of the beta/(beta + alpha) ratio is best represented by the low volume sample set because there is little alpha attenuation. The distribution can be "restored" by the application of correction factors to the alpha activity in the higher volume samples. There is little beta attenuation because the predominant beta activity is from either $^{90}Sr/^{90}Y$ or ^{137}Cs, both of which produce beta particles with energies high enough to be relatively unattenuated by the dust layer.

The adjusted distributions are compared to the low volume distribution with a goodness of fit test and the R^2 statistic (Gareth et. al. 2013) is computed. The highest R^2 value is used to select a correction factor. Figure 2 bottom left shows the corrected distribution, while bottom right shows the ratings of the other correction factor candidates.

The statistical analysis derives the correction factor with respect to volume (due to dust loading), but not the overall correction factor. The overall correction factor is obtained by scaling the dust loading correction factors by analytical laboratory results of lightly loaded samples and validated Monte Carlo simulations. The analytical laboratory dissolved the filters in acid, evaporated the liquid and counted a small enough extracted amount of the residue to avoid self-attenuation. These samples were then analyzed by alpha spectroscopy.

Monte Carlo simulations are performed using an MCNP model. To develop the MCNP correction factors, results are scaled against an ideal filter with all activity on top of the filter, with no attenuation from the filter or any dust loading. At early stages of sampling, when the dust loading is between 0.1 $mg \cdot cm^{-2}$ and 0.3 $mg \cdot cm^{-2}$, radioactivity is simulated to deposit at a depth distribution based on Geryes 2009-b. Dust particle dimensions are not modeled. Specifically, of the options provided in this reference, the data relating 3.7 μm AMAD particles, deposited in a glass fiber filter at 1 $m \cdot s^{-1}$ were selected. Modeled activity depths in the filter are provided in Table 1. The elemental composition of the model includes glass for the filter (elemental composition defined in Higby 1984), including light dust loading, and ordinary concrete (predominantly oxygen and silicon), for surface loading (elemental composition of "ordinary concrete NBS 04" defined in McConn et.al. 2011). The concrete definition was selected because it may be a true cause of dust in the bare, concrete-walled facility, but it would also be a reasonable approximation for silica clay dust.

The light dust loading details are not particularly important for establishing correction factors for higher levels of dust loading, but these results help validate the model; comparative models and studies of actual filters match the trends in results in this range (Geryes 2009-a,-c, and 2011). Specifically, the increase in correction factor between 0.1 and 0.3 $mg \cdot cm^{-2}$ shown in Table 2 is followed by a slight decrease, corresponding to typical filter behavior in which the filter is loaded at depth before surface loading begins. The MCNP model was further validated by comparing to an internal SRS study of alpha counts at various layers of polyethylene terephthalate†. The counting system used on the samples is combined alpha and beta with a discriminator setting. Alphas crossing the surface into the detector in the MCNP model were counted if they had at least 1.7 MeV energy to distinguish them from betas.

RESULTS

Figure 3 plots the results of the statistically derived correction factors (solid circles) and correction factors derived from the MCNP model. A solid line provides the results of a linear fit between 227 m^3 and 1024 m^3.

The MCNP results are added to Figure 3, with the 9 $mg{\cdot}cm^{-2}$ x-coordinate set equivalent to 1000 m^3. The MCNP results are shown as a dotted line consisting of a straight-line plot between 19 simulated levels of dust loading, starting at 0.1 $mg{\cdot}cm^{-2}$. The local maximum in the MCNP model is due to the early buildup of material in the filter, followed by later buildup on the top of the filter. When the activity begins to deposit on the top of the filter, alpha attenuation is briefly reduced since these most recent additions do not have to pass through the filter. With additional volume, the dust layer gets thicker on top of the filter, and eventually, the dust loading exceeds the maximum alpha range. The straight line starting point suggests that only alpha particles originating in approximately the top 2 $mg{\cdot}cm^{-2}$ of the dust layer are counted.

The linear regression is performed with R (R Dev 2010), and is shown for both the volume and areal density units (R^2=0.94). To account for the match-up of the MCNP data (which was based on known mass of dust loading) to the volumetric sample data, a mass concentration in the collected air is implied. The mass concentration was estimated to be 156 $\mu g{\cdot}m^{-3}$, based on scaling of the MCNP results. This is computed by dividing the mass on the filter (areal density multiplied by the filter area (pi times the 47 mm diameter squared)), then dividing by the volume. This computation is:

$$(9\ mg{\cdot}cm^{-2} \times 1000\ \mu g{\cdot}mg^{-2} \times (\pi \times (4.7\ cm/2)^2))/1000\ m^3$$

Figure 3 shows three distinct regions of interest. At the low level, correction factors do not have a linear relationship with dust loading; the correction factors start at a low level, then increase to a short plateau. At around 200 m^3, correction factors begin increasing linearly with volume. At greater than around 1000 m^3, the calculated correction factor remains about the same.

The correction factors in Figure 3 have been adjusted to start from a base of 1.2. This factor accounts for all other needed corrections including attenuation by the filter and particle self-attenuation. The factor of 1.2 is based on analytical laboratory results of lightly loaded samples, around 200-300 m^3. These samples were dissolved to eliminate attenuation issues and resulted in ratios to the filter counting system results at a ratio of around 1.4.

The resulting correction factors are:

† Internal SRS document, Dailey AE, Hadlock DJ, ESH-RPS-2007-00163, *Alpha Attenuation Due to Dust Loading*, August 2007.

1) At dust loading levels less than 11.1 m^3, (less than 0.1 $mg \cdot cm^{-2}$), the correction factor is 1.2.
2) At dust loading levels greater than this minimal loading but less than 185 m^3, (less than 1.7 $mg \cdot cm^{-2}$), the correction factor is 1.4.
3) At volumes between 185 m^3 and 1024 m^3, (1.7 $mg \cdot cm^{-2}$ to 9 $mg \cdot cm^{-2}$), a linear formula is provided to compute correction factors:
   $cf = 0.744 + 0.003533 \times \text{Volume } (m^3)$
   -or-
   $cf = 0.744 + 0.39255 \times \text{dust loading } (mg \cdot cm^{-2})$.
4) Samples with volumes greater than 1024 m^3, the correction factor is greater than 4.4.

Uncertainties in the derived correction factors are based on volume. They do not include the uncertainties in the volume and activity measurements and are based on the standard error of the linear regression in the linear portion of Figure 3. All uncertainties are presented at 1 σ. The slope has an uncertainty of 5.6%. The intercept uncertainty is 17%. The effect of these uncertainties, evaluated on the linear portion, provides a combined uncertainty of 11% at 227 m^3, decreasing gradually to 7.6% at 1024 m^3.

Uncertainty in converting the volume to dust loading may be estimated based on Type B uncertainties in modeling (Taylor and Kuyatt 1994). The uncertainty in the MCNP model, including the energy cutoff at 1.7 MeV, but excluding the dust composition, is roughly estimated at 5%. The dust loading material uncertainty is estimated to be 3% based on rerunning the MCNP model with elemental composition of the dust changed from concrete to air. This had a maximum effect, reducing the counts by 6%[‡]. Combining these two uncertainties results in a 1 σ uncertainty of 5.8%.

DISCUSSION

The linear range of Figure 3 represents steady-state sampling. In this range, a new layer of radioactive dust is being added which attenuates an equal layer of radioactive dust sampled earlier. The result is a constant alpha count rate over the linear range which requires a correction factor that increases consistently with the dust loading rate.

While the correction factor should be applied to high dust loading situations, it is crucial to realize that some data may be lost and that more recently collected particles will be much better represented than the particles collected earlier. If practical, it is much better to sample below the linear portion of Figure 3. Filters cannot be loaded indefinitely as demonstrated by the loss of material. The samples in this data set appear to have a maximum loading of around 9 $mg \cdot cm^{-2}$. Those experienced with collecting dusty samples will anecdotally attest to the visible loss of sample at collection time.

The dust loading is relatively high in the selected samples for a number of reasons. Air samples that have significant alpha activity are most likely from radiological areas that have limited access for

---

‡ A hand calculation based on Equation 5.21 of Cember 2009, in which the square roots of the effective atomic masses of the two compounds were used to estimate effective ranges, would have predicted an increase of 23% instead of the decrease of 6%.

cleaning. The facility was built in the 1950's, has bare concrete walls, and surfaces such as overhead piping and cable chases that are difficult to access, combined with fairly high ventilation rates. These conditions provide sufficient dust resuspension for the derived mass concentration of dust, 156 $\mu g \cdot m^3$, to be credible. This level of dust loading is in the range of air samples that were evaluated at SRS in predominantly nonradiological areas in 2010[§].

The statistical technique to derive correction factors provided reasonable results. Application to any other scenario has not been evaluated. Uncertainties described above are intended to provide the best available estimate of the correction factors evaluated for the data set, but should not be expected to apply to specific sample results.

CONCLUSION

A large set of air sample filter count data from a uranium and plutonium facility was evaluated based on the distribution of beta to total beta plus alpha activity in each sample compared to the volume of air recorded for each sample. A set of correction factors was developed based on this distribution. Comparison of the set of correction factors to what is known about the dust levels in the facility and Monte Carlo modeling provides corroboration of the results.

REFERENCES

Barnett JM, Cullinan VI, Barnett DS, Trang-Le TLT, Bliss M, Greenwood LR, and Ballinger MY, Results of a Self-Absorption Study on the Versapor 3000 47-mm Filters for Radioactive Particulate Air Stack Sampling, Health Phys 97:S161–S168; 2009.

Billard F, Madelaine G, Parnianpour H, Pénétrations des Aérosols dans les Filtres – Détermination de l'Autoabsorption, Proceedings of a Symposium, Vienna: Assessment of Airborne Radioactivity. International Atomic Energy Agency; IAEA-SM-95/11; 1967.

Cember J, Johnson TE, Introduction to Health Physics, 4th ed. New York: McGraw-Hill; 2009.

Gareth J, Witten D, Hastie T, Tibshirani R, An Introduction to Statistical Learning with Applications in R, New York, NY, Springer; 2013.

Geryes T, Monsanglant-Louvet C, Gehin E, Dégradation de la Mesure Nucléaire dans les Filtres pour les Prélèvements Atmosphériques; 2007. Thesis. IRSN- 2010-123.

Geryes T, Monsanglant-Louvet C, Gehin E, Effet de la taille des aérosols et de leur vitesse de filtration sur la dégradation de la mesure de l'activité des aérosols radioactifs émetteurs alpha prélevés sur filtre à fibres, 24ème Congrès Français sur les Aérosols; 2008.

Geryes T, Etude Expérimentale et Numériques de la Dégradation de la Mesure Nucléaires d'aérosols Radioactifs Prélevées avec des Filtres de Surveillance. Université Paris-Est, Faculté Des Sciences De Créteil; 2009-a. Thesis. IRSN-2010/123.

Geryes T, Monsanglant-Louvet C, Berger L, Gehin E, Application of the Monte Carlo Method to Study the Alpha Particle Energy Spectra for Radioactive Aerosol Sampled by an Air Filter, Health Phys 97:125–131; 2009-b.

[§] Internal SRS document, Smiley JJ, SRNS-J6700-2012-00181, *Dust Loading Studies at the Savannah River Site*, April 2012.

Geryes T, Monsanglant-Louvet C, Gehin E, Experimental and simulation methods to evaluate the alpha self-absorption factors for radioactive aerosol fiber filters, Radiat Meas 44: 763-765; 2009-c.

Geryes T, Monsanglant-Louvet C, Determination of Correction Factors for Alpha Activity Measurements in the Environment (Conditions of High Dust Loading), Radiat Prot Dosim 144: 659–662; 2011.

Goorley T, James M, Booth T, Brown F, Bull J, Cox LJ, Durkee J, Elson J, Fensin M, Forster RA, Hendricks J, Hughes HG, Johns R, Kiedrowski B, Martz R, Mashnik S, McKinney G, Pelowitz D, Prael R, Sweezy J, Waters L, Wilcox T, and Zukaitis T, Initial MCNP 6 Release Overview, Nucl Technol 180:298-315; 2012.

Huang S, Schery SD, Alcantara RE, Rodgers JC and Wasiolek P, Influence of Dust Loading on the Alpha-Particle Energy Resolution of Continuous Air Monitors for Thin Deposits of Radioactive Aerosols, Health Phys 83:884-891; 2002.

Higby DP, Effects of Particle Size and Velocity on Burial Depth of Airborne Particles in Glass Fiber Filters. Pacific Northwest Laboratories, PNL-5278; 1984.

Hinds WC, Aerosol Technology: Properties, Behavior, and Measurement of Airborne Particles, 1st ed. New York: John Wiley & Sons; 1999.

Hogue M, Thompson M, Farfan E, Hadlock D, Hand Calculations for Transport of Radioactive Aerosols through Sampling Systems, Health Phys 106:S78–S87; 2014.

Labone TR, Chalmers N, Applied Statistics and Data Analysis for Health Physics, Aiken SC: MJW Corp; 2014.

Luetzelschwab JW, Storey C, Zraly K, Dussinger D, Self-Absorption of Alpha and Beta Particles in a Fiberglass Filter, Health Phys 79:425-430; 2000.

Maiello ML, Hoover MD, Radioactive Air Sampling Methods, 1st ed. New York: CRC Press; 2011.

McConn RJ Jr, Gesh CJ, Pagh RT, Rucker RA, Williams RG III, Compendium of Material Composition Data for Radiation Transport Modeling, Pacific Northwest National Laboratories, PNNL-15870 Rev. 1; 2011.

Pickering S, The Interpretation of Alpha Energy Spectra from Particulate Sources, Journal of Aerosol Science 15(5):533-543; 1984.

Strom DJ, Joyce KE, MacLellan JA, Watson DJ, Lynch TP, Antonio CL, Birchall A, Anderson KK, Zharov PA, Disaggregating Measurement Uncertainty from Population Variability and Bayesian Treatment of Uncensored Results, Radiation Protection Dosimetry, 149(3):251–267; 2012.

Taylor BN, Kuyatt CE, Guidelines for Evaluating and Expressing the Uncertainty of NIST Measurement Results, Gaithersburg, MD: NIST; National Institute of Standards and Technology; Technical Note 1297; 1994.

The R Development Core Team, R: A Language and Environment for Statistical Computing Reference Index, Version 2.12.0; 2010.

Whicker J, Rodgers J, Moxley J, A Quantitative Method for Optimized Placement of Continuous Air Monitors, Health Phys. 85(5):599–609; 2003.

* Savannah River Nuclear Solutions, LLC, Bldg. 730-1B Rm. 108, Aiken, SC 29808

For correspondence, contact Mark Hogue, SRNS, Bldg. 735-2B Rm. 108, Aiken, SC 29808 or email at mark.hogue@srs.gov.

Figure Captions:

Figure 1: Distribution of activity ratios in a uranium and plutonium processing facility.

Figure 2: Matching activity ratio distributions by applying dust loading correction factor.

Figure 3: Derived dust correction factors by volume (m^3) and dust loading areal density ($mg \cdot cm^{-2}$). Note: vertical axis begins at 1.2 $mg \cdot cm^{-2}$.

Maximum Depth (cm)	Range above Maximum Depth (cm)	Activity Fraction
0.00434	0.00434	0.694444
0.00803	0.00369	0.138889
0.01147	0.00344	0.044192
0.01509	0.00362	0.022096
0.01878	0.00369	0.017045
0.02301	0.00423	0.015783
0.02725	0.00424	0.012626
0.03093	0.00368	0.012626
0.03461	0.00368	0.012626
0.04841	0.0138	0.029672

Table 1: MCNP model activity depth in filter

Total Dust, ($mg \cdot cm^{-2}$)	Top Layer Dust, ($mg \cdot cm^{-2}$)	Correction Factor = Ratio to Baseline
0 (baseline)	0	1.000
0.1	0	1.322
0.2	0	1.356
0.3	0	1.393
0.4	0.1	1.305
0.5	0.2	1.263
0.8	0.5	1.235
1.2	0.9	1.267
2	1.7	1.417
2.5	2.2	1.555
3	2.7	1.718
3.5	3.2	1.924
4	3.7	2.169
4.5	4.2	2.429
5	4.7	2.686
6	5.7	3.203
7	6.7	3.700
8	7.7	4.201
9	8.7	4.705

Table 2: MCNP air sample filter alpha count results

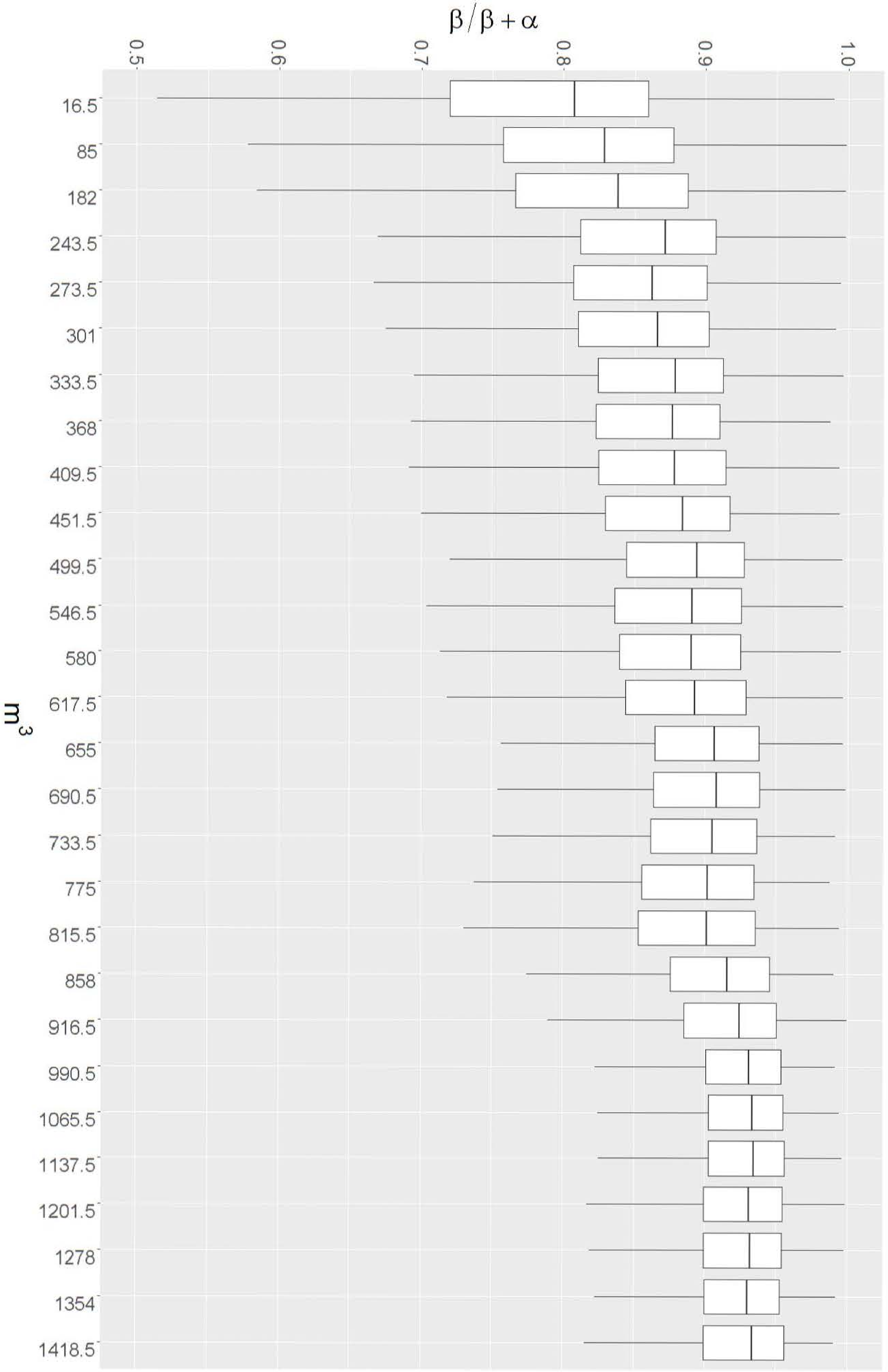

β/β+α
0.5
0.6
0.7
0.8
0.9
1.0
m3
16.5
85
182
243.5
273.5
301
333.5
368
409.5
451.5
499.5
546.5
580
617.5
655
690.5
733.5
775
815.5
858
916.5
990.5
1065.5
1137.5
1201.5
1278
1354
1418.5

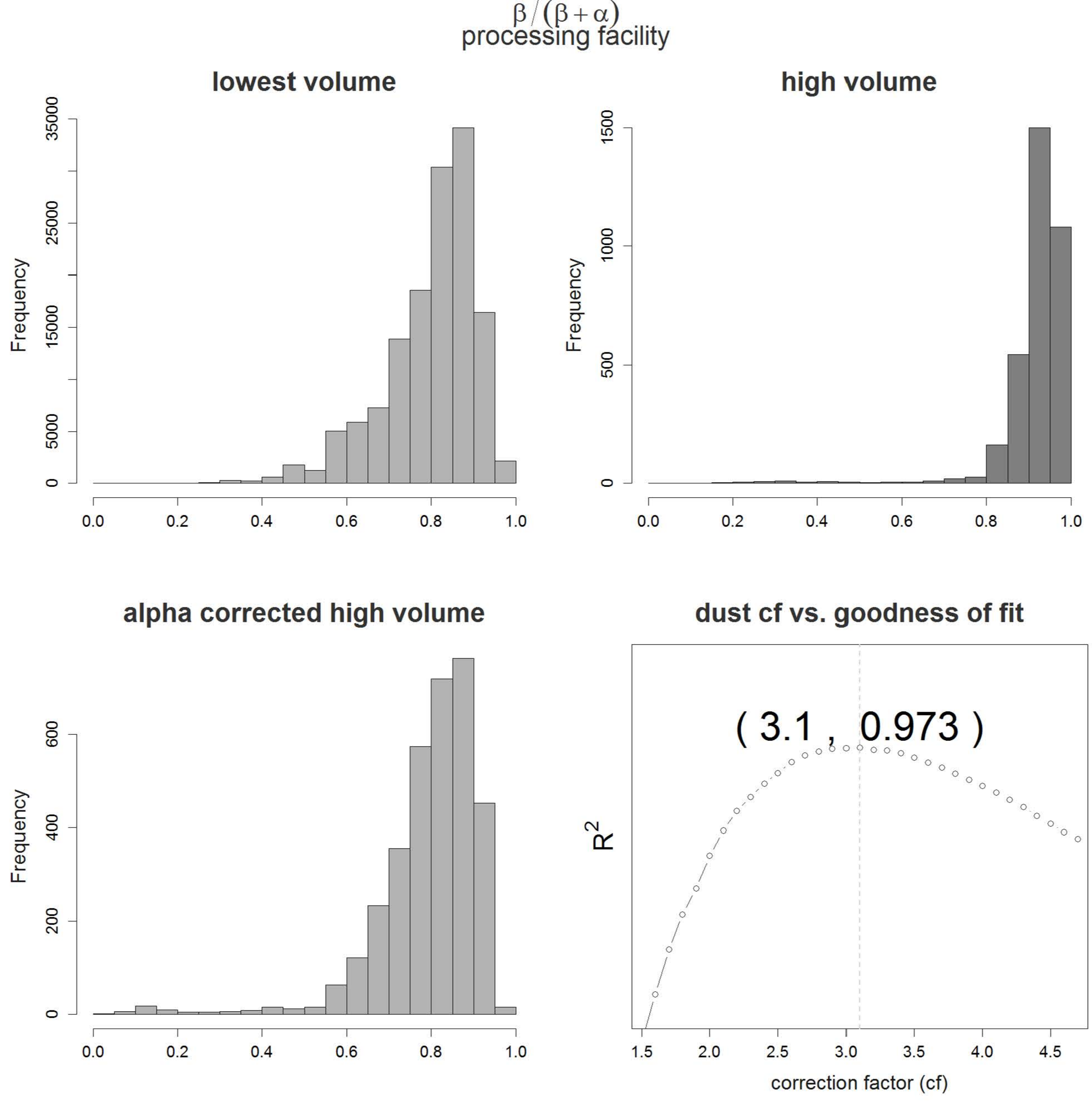

β/(β+α)
processing facility
lowest volume
high volume
alpha corrected high volume
dust cf vs. goodness of fit
Frequency
(3.1 , 0.973)
R2
correction factor (cf)

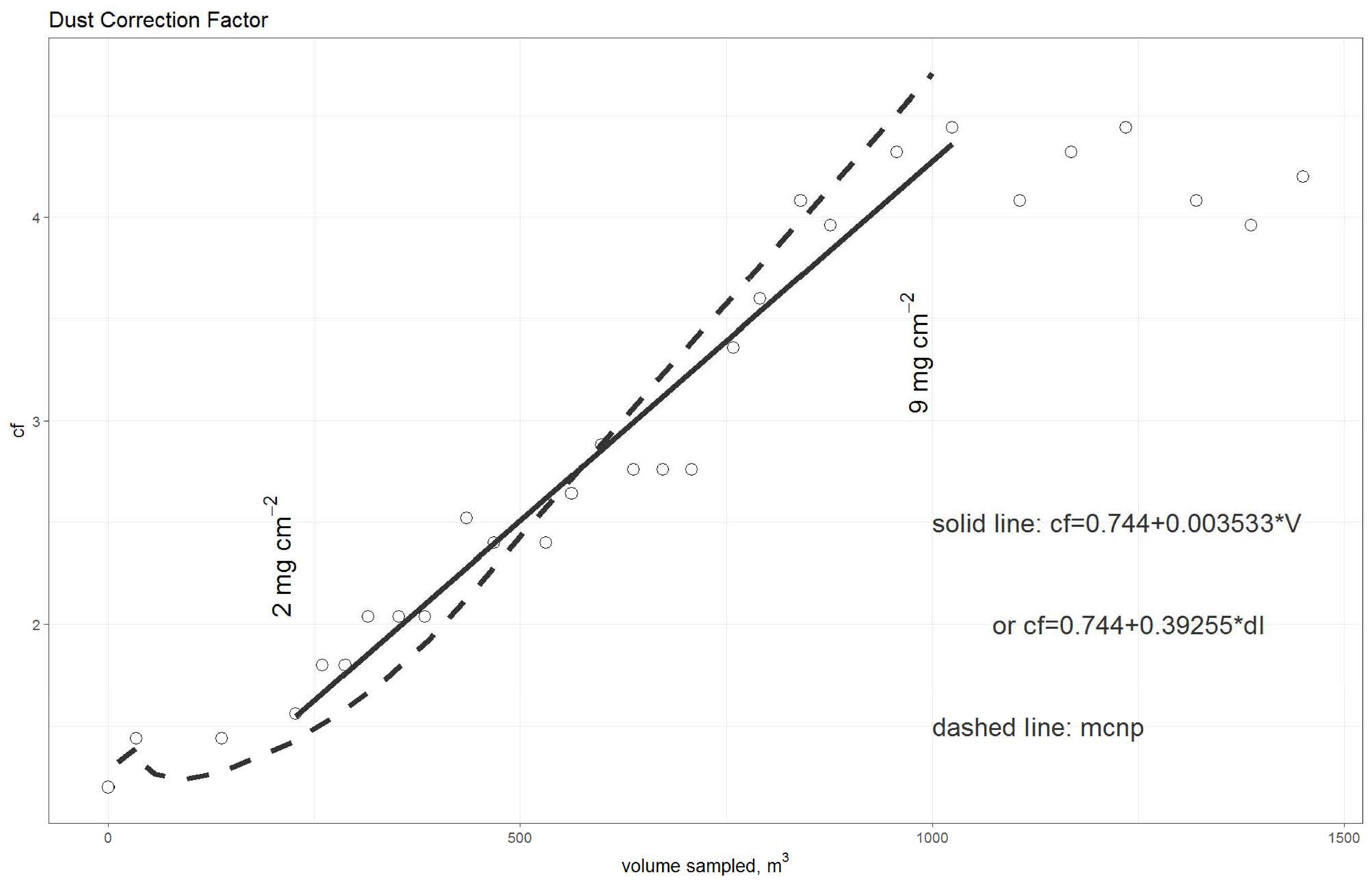

Dust Correction Factor
cf
4
3
2
0
500
1000
1500
volume sampled, m3
2 mg cm−2
9 mg cm−2
solid line: cf=0.744+0.003533*V
or cf=0.744+0.39255*dl
dashed line: mcnp